



Repositorio Institucional de la Universidad Autónoma de Madrid

<https://repositorio.uam.es>

Esta es la **versión de autor** del artículo publicado en:

This is an **author produced version** of a paper published in:

Journal of Physical Chemistry C 122.48 (2018): 27301-27313

DOI: <https://doi.org/10.1021/acs.jpcc.8b06142>

Copyright: © 2018 American Chemical Society

El acceso a la versión del editor puede requerir la suscripción del recurso

Access to the published version may require subscription

Theoretical Insights into Vinyl Derivatives Adsorption on a Cu(100) Surface

Fernando Aguilar-Galindo[†] and Sergio Díaz-Tendero^{*,†,‡,¶}

Departamento de Química - Módulo 13 - Universidad Autónoma de Madrid -28049 Madrid - Spain., Condensed Matter Physics Center (IFIMAC), Universidad Autónoma de Madrid -28049 Madrid - Spain., and Institute for Advanced Research in Chemical Sciences (IAdChem), Universidad Autónoma de Madrid -28049 Madrid - Spain.

E-mail: sergio.diaztendero@uam.es

Abstract

We present a thorough theoretical study of the adsorption of acrolein (ACO), acrylonitrile (ACN) and acrylamide (ACA) on a Cu(100) surface. To this, we have used the Density Functional Theory (DFT), imposing Periodic Boundary Conditions (PBC) to have a correct description of the electronic band structure of the metal, and including dispersion forces through two different schemes: the D2 method of Grimme and the vdW-DF. We have found several adsorption geometries; In all of them, the vinyl group together with the amide (in ACA), ciano (in ACN) and carbonyl (in ACO) groups, is highly involved. The highest adsorption energy is found for acrylamide, followed by acrolein and the lowest for acrylonitrile (depending on the level of theory employed $\sim 1.2, 1.0, 0.9$ eV respectively). We show that a strong coupling between the π electronic system (both occupied and virtual orbitals) and the electronic levels of the metal

*To whom correspondence should be addressed

[†]Chemistry-UAM

[‡]IFIMAC

[¶]IAdChem

is the main responsible of the chemisorption. As a consequence, electronic density is transferred from the surface to the molecule, whose carbon atoms acquire a partial sp^3 hybridization. Lone pair orbitals of the cyano, amide and carbonyl groups also play a role in the interaction. The simulations and following analysis allow to disentangle the nature of the interaction, which can be explained on the basis of a simple chemical picture: donation from the occupied lone pair and π orbitals of the molecule to the surface and backdonation from the surface to the π^* orbital of the molecule (π -backbonding).

Introduction

Adsorption of organic molecules on metal surfaces is a process of high interest due to the large number of technological applications in which it is involved: heterogeneous catalysis,¹⁻⁷ hybrid metal-organic materials,⁸⁻¹⁷ photovoltaic organic nanodevices,¹⁸⁻²¹ ultrathin optoelectronics,²²⁻²⁶ organic solar cells,^{19,21,27,28} molecular spintronics,²⁹⁻³² corrosion protectors,^{24,33-36} etc. The interaction of the organic molecules between them and with the substrate favours specific orientations, which can lead to formation of Self-Assembled Monolayers, SAMS.³⁷⁻⁴³ The coupling between the metal and the molecules in the SAMS causes the appearance of electronic properties that both parts do not present separately.⁴⁴ This is a key point of the hybrid materials. Furthermore, these surface-molecule interactions modify the electronic structure of the adsorbed molecules, weakening some chemical bonds and enhancing the reactivity, which can be applied in heterogeneous catalysis. In the adsorption, some organic groups are specially involved. Though, the molecule-substrate affinity does not depend only on the group, but also on the nature of the surface (chemical composition and topology), as well as on the conjugation or proximity to other groups in the molecule. Acrolein, acrylonitrile and acrylamide present different groups and are thus excellent candidates to study the interaction between organic molecules and metal surfaces (see structures in Fig. 1). These molecules are polymer precursors, reason why they have an important technological interest. Their common structural characteristic is the presence of a vinyl group,

with a double C=C bond, which is usually involved in strong adsorptions (chemisorption) with the surface.^{45,46} This bond is conjugated with different functional groups in each of the three molecules, so they can be used to study how the electronic delocalization due to conjugation affects a substituted alkene interacting with a metal surface, and its adsorption ability.

Experimental works on similar molecules adsorbed on Cu(100) surface have been carried out: Temperature-programmed desorption and near-edge X-ray absorption techniques were used to study the decomposition reactions to generate vinyl groups from vinyl bromide and vinyl iodide on Cu(100);⁴⁷ The same techniques were used to study the bonding and reactivity of allyl groups (CH_2CHCH_2) on a Cu(100) surface;⁴⁸ And more recently, combination of temperature-programmed reaction/desorption and reflection-absorption infrared spectroscopy was employed to study reactions of $\text{CH}_2 = \text{CHBr}$ and CH_3CHBr_2 on Cu(100).⁴⁹ Linking of the vinyl group to the surface is a key aspect to understand the reactivity of these experiments.

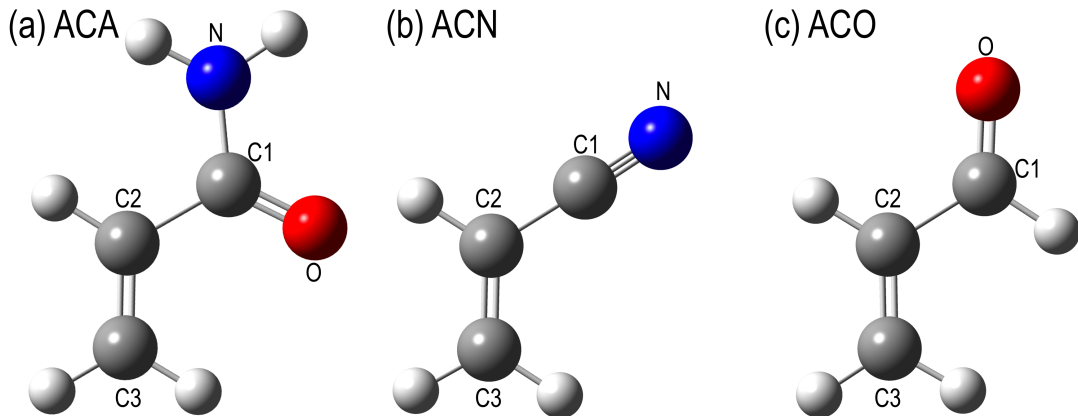


Figure 1: The three vinyl derivative molecules studied in the present work: (a) acrylamide (ACA), (b) acrylonitrile (ACN), and (c) acrolein (ACO). Labels of atoms in each molecule correspond to those used in Tables 1, 2 and 3.

Over the last decades, different experimental techniques have been developed to probe properties of adsorbed molecules (as adsorption energy and geometry, electronic and vibrational levels, etc.). Adsorption geometries can be measured with high precision using atomic

force microscopy (AFM)^{50,51} or scanning tunneling microscopy (STM),⁵²⁻⁵⁴ being this last technique able to study also the electronic structure near the Fermi level. X-ray standing wave (XSW)⁵⁵ is an extremely powerful technique for obtaining information of surfaces and interfaces on the atomic scale, by combining diffraction with other spectroscopic techniques. PhotoElectron Diffraction (PED)^{56,57} takes advantage of the scattering response of photoexcited electrons to obtain accurate information on the structural information on surfaces. The strength of the molecule-surface interaction (adsorption energy) can be obtained through temperature programmed desorption (TPD)^{58,59} experiments. X-ray spectroscopy^{60,61} allows to evaluate the change in the electronic density associated to charge transfer processes or changes in the vicinity of the atoms due to new formed bonds. Nevertheless, although these methods provide valuable data, the interpretation of the results is sometimes difficult and theoretical calculations arise as an excellent approach to help in the interpretation of experimental measurements. Also, the study of some properties is a real challenge from the experimental point of view, whereas by means of theoretical simulations this information can be obtained.

From a fundamental point of view, the theoretical description of these systems is a challenge,⁶² in particular their electronic structure: whereas metals have a continuum energy spectrum, molecules present discrete levels. The interaction of the two subsystems causes a coupling of the electronic levels, which generates charge transfer processes and gives a certain lifetime to the molecular states, becoming resonances (discrete levels immersed in a continuum).⁶³⁻⁶⁷ Another issue to describe the interaction between organic molecules and metal surfaces is that this process is frequently ruled by weak interactions.⁶⁸⁻⁷⁴ These forces are crucial in certain cases, in particular when in the adsorption process covalent bonds are not formed and molecule and surface keep their previous identities (physisorption). This kind of interactions (as dispersion or Van der Waals forces) is related with the so-called “dynamic” electronic correlation. There are some alternatives to recover this correlation, as the Configuration Interaction (CI) methods or the ones based in perturbation theory (MPn

family). Nevertheless, all these post-Hartree-Fock methods require a huge computational effort so their use is restricted to small systems. As an alternative, it is possible to use Density Functional Theory (DFT). This methodology scales much better than the post Hartree-Fock methods, so it can be used for larger systems (hundreds of atoms) with an affordable computational time. The different methods developed for including dispersion forces in DFT can be clasified in three families: (i) A pairwise-additive correction to the total energy, proposed by Grimme.⁷⁵⁻⁷⁷ In these methods the dispersive energy is described by damped interatomic potentials of the form $C_6 R^{-6}$. (ii) The Van-der-Waals density functionals (vdW-DF) are density derived methods^{78,79} that explicitly include in the Hamiltonian a non-local functional of the electron density to account for the dispersion forces; optPBE-vdW⁸⁰ and vdW-DF-cx^{81,82} are successful implementations of this family. (iii) The third family merge the ideas of the two previous ones; i.e. the methods in this category compute the vdW parameters such as atomic C_6 coefficients, vdW radii R , and static atomic polarizabilities α_0 as functionals of the chemical environment and the electron density. Robust developments of this idea are the DFT+XDM approach⁸³⁻⁸⁵ originally proposed by Becke and Johnson, and the DFT+vdW approach of Tkatchenko and Scheffler.⁸⁶ In the review⁸⁷ an exhaustive analysis of the use of these methods for the description of hybrid inorganic/organic systems can be found. We compare results obtained with the D2 method⁷⁶ and with the optPBE functional.⁸⁰

In this work, we present a Density Functional Theory study of the absorption of acrolein, acrylonitrile and acrylamide on a pristine Cu(100) surface. Density Functional Theory has been probed to give excellent results in the description of interactions between organic molecules and metal surfaces (see e.g.^{45,70,73,74,88-92}). Although in the study of isolators, cluster models are usually good enough to describe correctly the electronic distribution of the system, in the case of metals finite clusters are not adequate, since the spatial confinement of the electronic density produces a spurious quantization of the electronic levels that is not present in the real metal. To avoid this, periodicity must be taken into account and

we introduce it by imposing Periodic Boundary Conditions (PBC) in our simulations. We first present a comparison between different approaches to include weak interactions, which are not taken into account in most of the DFT functionals. Then, we deepen in the understanding of the adsorption process, through the analysis of the changes in the electronic levels of the molecule (coupling with the metallic continuum and shifting in the energy spectrum), as well as the study of the transferred charge (value and spatial distribution) due to the interaction. The thorough theoretical analysis here presented, allows to characterize the nature of the interaction between the molecules and the metal surface.

Computational details

All the calculations were done in the framework of the Density Functional Theory (DFT) using the Vienna Ab initio Simulation Package (VASP),^{93,94} which uses Periodic Boundary Conditions (PBC). The use of PBC is required in order to describe the metallic character of the surface. The exchange-correlation (XC) potential was calculated in the generalized gradient approximation (GGA), using the Perdew-Burke-Ernzerhof (PBE)⁹⁵ functional. The interaction between ions and electrons has been described through the projector augmented wave (PAW) pseudopotentials of the VASP database. The electronic density is expanded in a plane wave basis set up to a kinetic energy cutoff of 750 eV, value for which convergence of absolute energy is reached. The periodic supercell contains a metal slab made by a four-layer (5×5) surface unit cell of copper atoms, the adsorbed molecule and a vacuum distance of ~ 20 Å in the direction perpendicular to the surface, defined as z -axis. The size of the supercell makes the interaction of the molecule with the z -closest replica surface negligible (for practical purposes, vacuum is imposed along this direction). The cell is big enough in the x, y directions to neglect also the interactions with the molecules of the replicas, so we work in the low-coverage regime, since single molecule adsorption is considered.

To sample the Brillouin zone, which is strongly related with the computational effort that

the calculation requires and the quality of the results, we used the Γ -centered Monkhorst-Pack scheme, with two different meshes: $1 \times 1 \times 1$ (only Γ -point) and $3 \times 3 \times 1$. This gives us three levels of theory, used to find a good compromise between computation time and accuracy:

- (1) Use of Γ -point only to optimize the geometry. Also, the energy is obtained at this level.
- (2) Single point with the $3 \times 3 \times 1$ mesh on the top of the Γ -point optimized geometry, denoted as “331/ Γ ”.
- (3) Geometry and energy obtained with the $3 \times 3 \times 1$ K-points mesh.

In the optimization calculations, a first-order Methfessel-Paxton scheme was used, with a σ value of 0.2 eV. In the extraction of the Partial Density Of States (PDOS) a gaussian smearing with a σ value of 0.1 eV was used. The electronic self-consistent convergence was set to 10^{-5} eV in order to have accurate energies and gradients. For the convergence criteria in the optimization, we impose all the Hellmann-Feynman forces to be lower than 0.005 eV \AA^{-1} for the geometrical coordinates that we allow to relax (x, y, z of the atoms in the molecule and the z coordinate of the atoms in the first layer of the metal surface).

We have explored the influence of weak interactions (e.g. Van der Waals forces), which are important to describe accurately geometries and energies in adsorption processes, in two different ways:

- DFT-D2 method of Grimme.⁷⁶ To avoid the overestimation of the dispersion energies, we included the Grimme’s scheme only in the molecule and in the first layer of the metal. This approach has been successfully used in the past.^{73,74}
- Inclusion of these interactions in the exchange-correlation functional, through the use of the optPBE functional.^{78–80,96}

We have checked the importance of relaxing the geometry of the second layer of Cu atoms. To this we have reoptimized the geometry all studied structures including geometry relaxation of the first two layers using the optPBE functional and a $1 \times 1 \times 1$ K-mesh (only Γ -point). Single point energy calculations were done over the new optimized geometry using the same functional and a $3 \times 3 \times 1$ K-points mesh. Adsorption energies are typically $\sim 1\%$ larger than in those cases where only one layer of Cu atoms was relaxed (always smaller than 5% in all cases). Relevant distances between atoms in the molecule-metal surface interaction barely change: for instance the distances between the carbon atoms of the vinyl group and the Cu atoms in the surface typically change in 0.005 Å, and never more than 0.013 Å, for the most stable structure found in each molecule.

To analyze the charge transfer, we have used the Quantum Theory of Atoms in Molecules (QTAIM) by Bader,^{97,98} with the code developed by Henkelman et al.⁹⁹⁻¹⁰¹

The initial geometries were chosen by placing functional groups of the molecules on top, bridge and hollow positions of the Cu(100) surface. Due to the high symmetry of the surface, different rotations and translations were considered as initial guess of the geometry to include several kinds of interactions in the exploration of the potential energy surface. In particular, for acrylonitrile we selected two initial guess geometries corresponding to those previously described in the literature.^{45,102-104} They show interactions between the C=C bond and the C \equiv N bond with the metal surface in two different orientations. For acrolein we started from different positions of the C=C bond: top, bridge and with carbon C3 on top. We combine these positions with different rotations to maximize other possible interactions of the molecule with the substrate. In the case of the acrylamide rotation of the molecule keeping the C=C bond on top, leads to three possible interactions: (i) O and N on top, (ii) O and C-N on bridge (iii) O and C-N on top. We also considered the case with C3 on top and O on bridge.

Results and discussion

We present the obtained results in four sections analyzing different aspects: adsorption geometries, interaction energies, charge transfer and changes in the electronic structure and bonding.

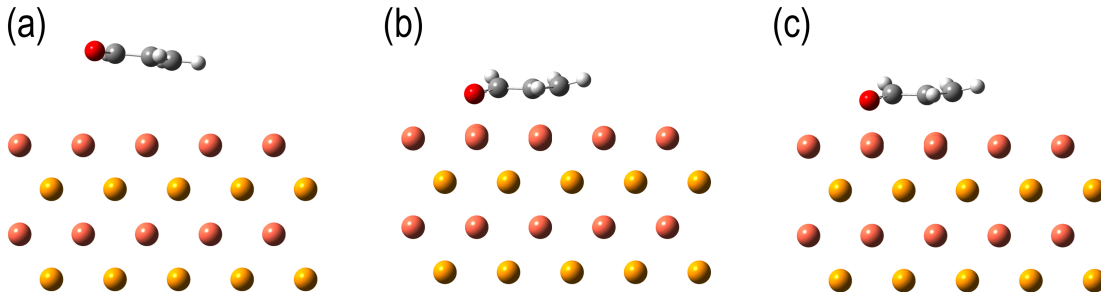


Figure 2: Side view of an optimized structure of acrolein adsorbed on a Cu(100) surface, obtained with (a) PBE, (b) PBE+D2, (c) OPTPBE. Two colors for the two different relative orientations of Cu layers are used.

Geometry

We first analyze the effect of introducing Van der Waals forces to study the geometry of adsorbed molecules on metal surfaces. To this, starting from the same initial geometry we optimized acrolein on Cu(100) at level 1 (Γ point) using the pure PBE -without Van der Waals corrections-, PBE+D2 and OPTPBE functionals. The lateral views after geometry optimization are shown in Fig. 2. The geometry changes dramatically if weak interactions are not included (the molecule-surface distance is increased by 2 \AA) and, accordingly, the adsorption energy is much smaller (52 meV at a 331/ Γ level). We thus corroborate that including weak interactions is crucial to study adsorption of organic molecules on a metal surface.

After the search of possible adsorption possibilities starting with different initial geometries with the previously explained strategy, we have found two minima for the adsorption of acrylamide on Cu(100), structures “ACA-1” and “ACA-2” (see Fig. 3); also, two for acrylonitrile

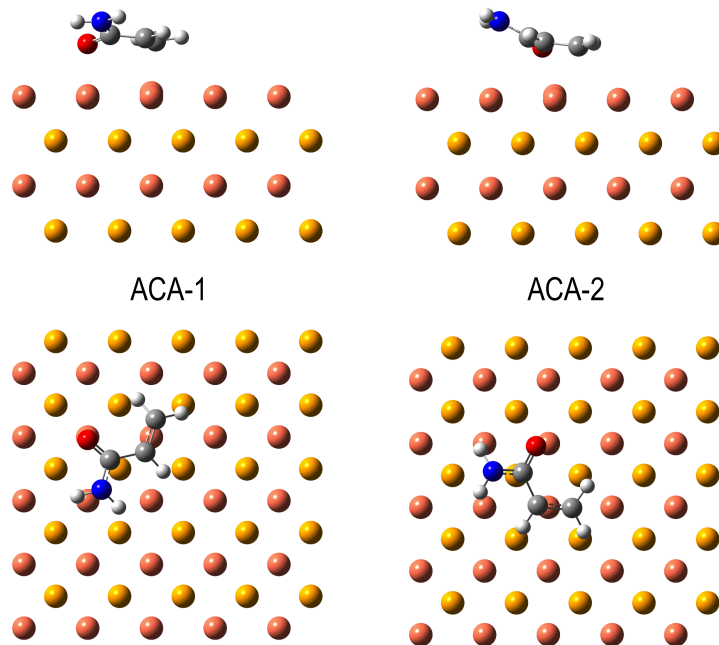


Figure 3: Top and side view of the two minima found for acrylamide adsorbed on a Cu(100) surface. Two colors for the two different relative orientations of Cu layers are used.

(“ACN-1” and “ACN-2”, Fig. 4); and three for acrolein (“ACO-1”, “ACO-2” and “ACO-3”, Fig. 5). Since the methods that include VdW forces, Grimme’s D2 and OPTPBE, provide very close geometries, regardless of the K-points mesh used in the optimization, with negligible differences at sight, we only show in the figures those obtained geometries using the OPTPBE functional.

In the adsorption of acrylamide, the oxygen atom interacts directly with one copper atom of the surface, placed on top position in both adsorption geometries. A second common characteristic in both cases is the location of the double C=C bond, also on top position. The main difference between ACA-1 and ACA-2 is the planarity of the molecule: in ACA-2 the nitrogen is further from the plane defined by the double C=C bond and the oxygen atom, with the amino group pointing towards the vacuum. The reason is that in ACA-1 the molecule–surface linkage is mainly localized on the oxygen atom (a strong σ O–Cu interaction is observed as detailed below), while in ACA-2 the Cu–C distance is lower than in ACA-1, showing that the interaction through the double C=C bond has a greater

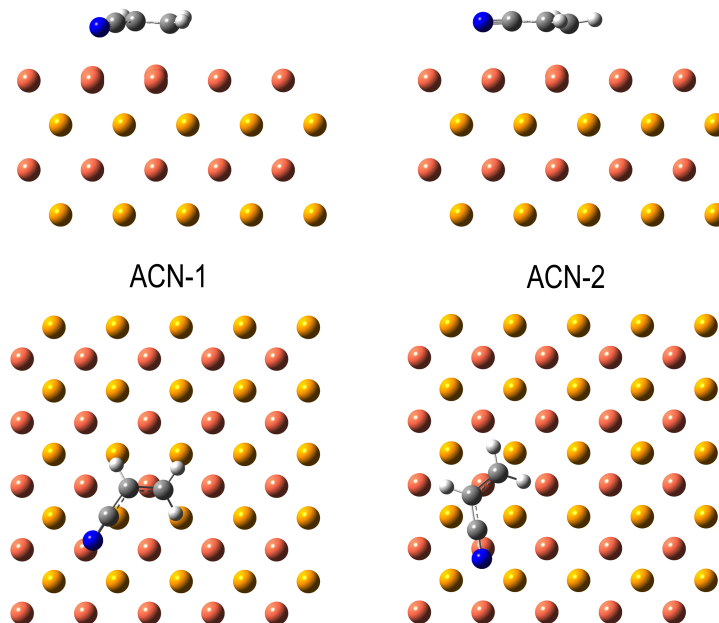


Figure 4: Top and side view of the two minima found for acrylonitrile adsorbed on a Cu(100) surface. Two colors for the two different relative orientations of Cu layers are used.

importance (as we will show below charge transfer to the π_{CC}^* orbital occurs). In a simple chemical picture, the carbon atoms would acquire stronger sp^3 character in ACA-1. Thus, the $-NH_2$ group points out the surface explaining the difference observed after geometry optimization. The electronic structure analysis provides further details and confirms the validity of this picture.

As in the case of acrylamide, the two minima found in acrylonitrile exhibit a clear direct interaction between the double $C=C$ bond and a copper atom of the first layer. The main difference between both structures is the relative orientation of the molecule on the surface, which determines the copper atoms that interact with the molecule. While in ACN-1 the nitrogen atom is located in top position, in ACN-2 the $C\equiv N$ bond interacts with the Cu atom. The relative orientation in ACN-1 makes also possible an interaction between the carbon atom of the cyano and a copper atom located in the second layer (in hollow position respect the first layer). In ACN-2, the two copper atoms of the first layer that interacts with the molecule are closer, so there is no hollow position available, and the molecule does

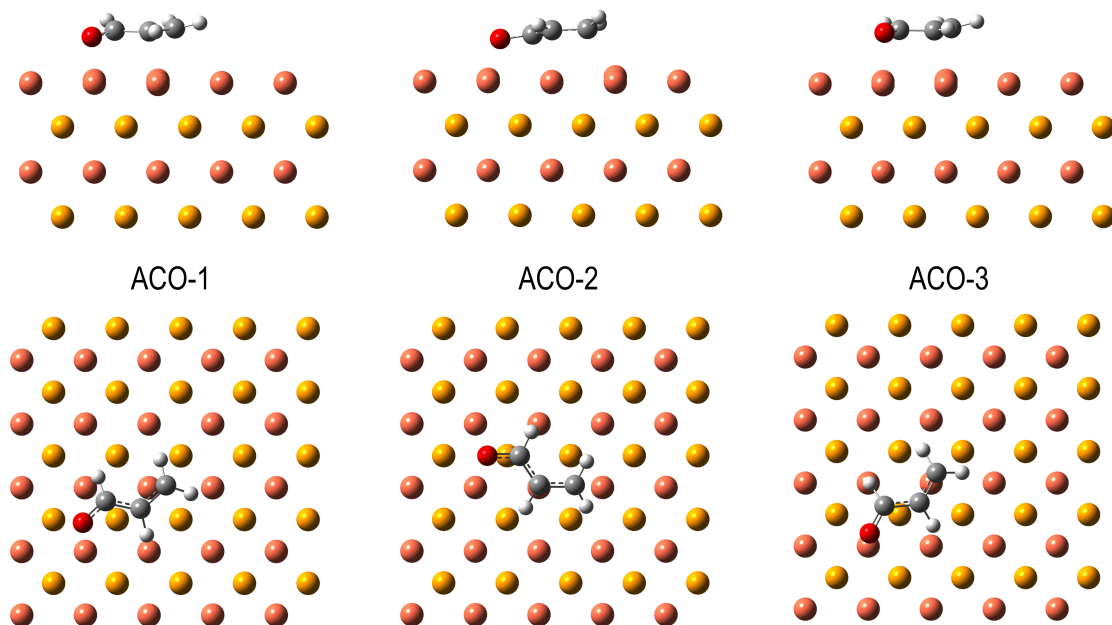


Figure 5: Top and side view of the three minima found for acrolein adsorbed on a Cu(100) surface. Two colors for the two different relative orientations of Cu layers are used.

not interact with atoms of the second layer. In ACN the hydrogen atoms also go out of the molecular plane and the carbon atoms do not have anymore a pure sp^2 hybridization. These geometrical distortions point out chemisorption, as detailed below.

Acrolein shows three different adsorption possibilities. ACO-1 and ACO-2 do not show the C=C bond in top position. The relative orientation of the C=O bond with respect to the surface in ACO-2 indicates that the local molecular dipole of this bond is pointing towards the surface, thus interacting in an electrostatic manner with the substrate rather than with a chemical bond. ACO-3 keeps the C=C as well as the oxygen atom in top position. ACO-1 has its oxygen atom in bridge position and also pointing to the surface, thus the dipole of the molecule plays a role in this adsorption geometry. As in the other two systems, sp^3 character is observed in the C atoms of the three adsorption geometries. This indicates that the interaction is not either pure dispersion in this case, but also shows some covalent character, chemisorption.

More detailed information on the geometry is presented in Tables 1, 2 and 3; bond

Table 1: Most relevant distances, in Å, of the minima found for acrylamide adsorbed on a Cu(100) surface after geometry optimization at the different levels of theory employed. Gas phase distances are also included for comparison.

| | | PBE+D2 | | OPTPBE | |
|-------|-------|--------|-------|--------|-------|
| | | Γ | 331 | Γ | 331 |
| ACA | C1-N | 1.371 | 1.371 | 1.375 | 1.375 |
| | C1-O | 1.234 | 1.234 | 1.236 | 1.236 |
| | C1-C2 | 1.495 | 1.495 | 1.496 | 1.496 |
| | C2-C3 | 1.336 | 1.336 | 1.336 | 1.336 |
| ACA-1 | C1-N | 1.358 | 1.359 | 1.360 | 1.361 |
| | C1-O | 1.274 | 1.273 | 1.272 | 1.271 |
| | C1-C2 | 1.461 | 1.462 | 1.466 | 1.468 |
| | C2-C3 | 1.409 | 1.405 | 1.394 | 1.389 |
| | C1-Cu | 2.718 | 2.729 | 2.788 | 2.804 |
| | C2-Cu | 2.183 | 2.203 | 2.310 | 2.376 |
| | C3-Cu | 2.136 | 2.153 | 2.212 | 2.237 |
| | N-Cu | 3.040 | 3.052 | 3.166 | 3.171 |
| ACA-2 | O-Cu | 2.066 | 2.081 | 2.107 | 2.124 |
| | C1-N | 1.359 | 1.361 | 1.360 | 1.361 |
| | C1-O | 1.277 | 1.278 | 1.273 | 1.273 |
| | C1-C2 | 1.456 | 1.454 | 1.464 | 1.464 |
| | C2-C3 | 1.424 | 1.421 | 1.404 | 1.401 |
| | C1-Cu | 2.819 | 2.797 | 2.911 | 2.923 |
| | C2-Cu | 2.112 | 2.126 | 2.222 | 2.239 |
| | C3-Cu | 2.183 | 2.210 | 2.225 | 2.267 |
| | N-Cu | 3.237 | 3.186 | 3.415 | 3.447 |
| | O-Cu | 2.071 | 2.093 | 2.106 | 2.137 |

Table 2: Most relevant distances, in Å, of the minima found for acrylonitrile adsorbed on a Cu(100) surface after geometry optimization at the different levels of theory employed. Gas phase distances are also included for comparison.

| | | PBE+D2 | | OPTPBE | |
|-------|-------|----------|-------|----------|-------|
| | | Γ | 331 | Γ | 331 |
| ACN | C1-N | 1.169 | 1.169 | 1.167 | 1.167 |
| | C1-C2 | 1.424 | 1.424 | 1.427 | 1.427 |
| | C2-C3 | 1.342 | 1.342 | 1.342 | 1.342 |
| ACN-1 | C1-N | 1.190 | 1.189 | 1.186 | 1.185 |
| | C1-C2 | 1.401 | 1.401 | 1.403 | 1.404 |
| | C2-C3 | 1.421 | 1.420 | 1.406 | 1.403 |
| | C1-Cu | 2.749 | 2.776 | 2.771 | 2.802 |
| | C2-Cu | 2.218 | 2.242 | 2.386 | 2.435 |
| | C3-Cu | 2.135 | 2.151 | 2.211 | 2.242 |
| | N-Cu | 2.063 | 2.071 | 2.101 | 2.110 |
| ACN-2 | C1-N | 1.188 | 1.188 | 1.181 | 1.181 |
| | C1-C2 | 1.411 | 1.410 | 1.415 | 1.416 |
| | C2-C3 | 1.409 | 1.409 | 1.395 | 1.392 |
| | C1-Cu | 2.359 | 2.348 | 2.500 | 2.517 |
| | C2-Cu | 2.183 | 2.206 | 2.293 | 2.333 |
| | C3-Cu | 2.174 | 2.179 | 2.264 | 2.295 |
| | N-Cu | 2.243 | 2.268 | 2.377 | 2.426 |

Table 3: Most relevant distances, in Å, of the minima found for acrolein adsorbed on a Cu(100) surface after geometry optimization at the different levels of theory employed. Gas phase distances are also included for comparison.

| | | PBE+D2 | | OPTPBE | |
|-------|-------|----------|-------|----------|-------|
| | | Γ | 331 | Γ | 331 |
| ACO | C1-O | 1.225 | 1.225 | 1.226 | 1.226 |
| | C1-C2 | 1.471 | 1.471 | 1.472 | 1.472 |
| | C2-C3 | 1.342 | 1.342 | 1.342 | 1.342 |
| ACO-1 | C1-O | 1.311 | 1.309 | 1.302 | 1.294 |
| | C1-C2 | 1.436 | 1.435 | 1.440 | 1.441 |
| | C2-C3 | 1.416 | 1.410 | 1.407 | 1.405 |
| | C1-Cu | 2.258 | 2.267 | 2.343 | 2.426 |
| | C2-Cu | 2.114 | 2.156 | 2.177 | 2.235 |
| | C3-Cu | 2.160 | 2.164 | 2.212 | 2.200 |
| | O-Cu | 2.098 | 2.111 | 2.113 | 2.089 |
| ACO-2 | C1-O | 1.332 | 1.333 | 1.330 | 1.333 |
| | C1-C2 | 1.424 | 1.418 | 1.426 | 1.419 |
| | C2-C3 | 1.448 | 1.456 | 1.443 | 1.455 |
| | C1-Cu | 2.379 | 2.390 | 2.447 | 2.447 |
| | C2-Cu | 2.069 | 2.099 | 2.112 | 2.138 |
| | C3-Cu | 2.180 | 2.158 | 2.246 | 2.190 |
| | O-Cu | 2.114 | 2.135 | 2.139 | 2.142 |
| ACO-3 | C1-O | 1.289 | 1.291 | 1.284 | 1.285 |
| | C1-C2 | 1.443 | 1.441 | 1.445 | 1.443 |
| | C2-C3 | 1.410 | 1.410 | 1.404 | 1.404 |
| | C1-Cu | 2.387 | 2.414 | 2.518 | 2.547 |
| | C2-Cu | 2.175 | 2.200 | 2.243 | 2.265 |
| | C3-Cu | 2.128 | 2.139 | 2.184 | 2.200 |
| | O-Cu | 2.032 | 2.036 | 2.061 | 2.066 |

distances have been extracted after the optimization at the different levels of theory for the three molecules. For comparison, we also include those of the isolated molecules in the gas phase. At the light of the numbers, the first conclusion is that the way in which the dispersion forces are included does not change the geometry of the molecule (bond distances barely change ~ 0.01 Å), but it affects the surface-molecule distances, where values can differ up to ~ 0.2 Å). The surface-molecule distances are usually underestimated when the D2 correction is included because this method lacks of screening effects inside the metal and thus, it overestimates the molecule-surface interactions. Nevertheless, since the C_6 parameter of the atoms in the molecules (H, C, N, O) are much lower than the one of Cu (0.14-1.75 *vs.* 10.82), the D2 correction has a small effect in the molecule. However, screening of dispersion interactions within the metal does not always lead to an increase in the molecule-surface distances. Since the screening reduces effective C_6 coefficients and vdW radii, distances can be significantly reduced by screening. This have been observed when comparing the Tkatchenko-Scheffler vdW method and the correctly screened vdW^{surf} method.^{87,105} We also realize that the changes when one increases the K-mesh from Γ to $(3 \times 3 \times 1)$ are almost negligible; A 331 optimization requires a huge computational effort and barely change the atomic positions. Since the supercell in the real space is quite large, its small reciprocal space is small enough to be accurately described with a single k-point. Regardless of the functional and k-mesh it is possible to appreciate common trends in the bond distances. In any molecule and adsorption geometry, the C1-C2 distance decreases after the interaction, whereas C2-C3 and C1- X ($X=\text{N}$ for ACN, and $X=\text{O}$ for ACA and ACO) get larger. This is what one would expect in case of population of the LUMO orbital, which has a bonding character between C1 and C2, and antibonding between C2 and C3 and between C1 and X . As we show below, in the LUMO region of the molecule an increase of the electronic density is indeed appreciated due to the interaction between the molecule and the surface, which also explains the sp^3 character of the C atoms involved in the bonding.

Adsorption energies

The adsorption energy is defined as:

$$E_{ads} = E_{mol/surface} - (E_{mol} + E_{surface}) \quad (1)$$

Where $E_{mol/surface}$ is the energy of the whole molecule+surface system, E_{mol} is the energy of the optimized molecule in the gas phase and $E_{surface}$ is the energy of the isolated bare surface. The results of the adsorption energies for all the studied structures, computed with the different levels of theory here considered, are shown in Table 4.

Table 4: Adsorption energies (in eV) of the acrylamide, acrylonitrile and acrolein on Cu(100) computed at the different levels of theory and with the two functionals employed.

| E_{ads} (eV) | | | | | | |
|----------------|-------------------|--------|-------------------|--------|--------------|--------|
| | (1) Full Γ | | (2) 331/ Γ | | (3) Full 331 | |
| | PBE+D2 | OPTPBE | PBE+D2 | OPTPBE | PBE+D2 | OPTPBE |
| ACA-1 | -1.225 | -0.930 | -1.154 | -0.879 | -1.157 | -0.879 |
| ACA-2 | -1.240 | -0.932 | -1.157 | -0.872 | -1.157 | -0.868 |
| ACN-1 | -0.940 | -0.644 | -0.856 | -0.590 | -0.882 | -0.601 |
| ACN-2 | -0.809 | -0.525 | -0.774 | -0.483 | -0.780 | -0.496 |
| ACO-1 | -1.063 | -0.736 | -0.980 | -0.674 | -0.995 | -0.696 |
| ACO-2 | -1.019 | -0.677 | -0.992 | -0.670 | -1.006 | -0.687 |
| ACO-3 | -1.056 | -0.740 | -0.998 | -0.701 | -1.006 | -0.704 |

The obtained values after the use of only the Γ -point and the single point $3 \times 3 \times 1$ on the top of the Γ -point geometry show that Γ -point is not enough to have correct energies. In particular, by using the PBE+D2 functional, adsorption energies change in average 63.0 meV, with a maximum difference of 84.0 meV. OPTPBE is however less affected by the different K-Point mesh: in average, the adsorption energy changes in 45.0 meV, with a maximum change of 62.0 meV. Nevertheless, the obtained results with levels (2) and (3) are very similar. The largest difference in adsorption energies from $3 \times 3 \times 1/\Gamma$ to full $3 \times 3 \times 1$ is 26.0 meV (PBE+D2) and 22.0 meV (OPTPBE). Average differences in adsorption energies do not change much either between levels (2) and (3): 10.3 meV (PBE+D2) and 10.0 meV

(OPTPBE). This indicates, as we have mentioned before, that the geometries obtained with Γ -point are almost the same than the ones provided by the $3 \times 3 \times 1$ mesh, but with an important gain in computational effort. Therefore, we conclude that the best compromise between accuracy and computational time is the $3 \times 3 \times 1/\Gamma$ level. If one compares the absolute adsorption energy of the most stable structure in each molecule at the $3 \times 3 \times 1/\Gamma$ and full $3 \times 3 \times 1$ levels (see Table 4), it can be seen that changes are 0 meV (ACA-1), 11meV (ACN-2) and 22meV (ACO-1).

Table 4 shows that, except in the case of the acrylonitrile, the different adsorption structures are almost degenerate in energy, regardless of the method used to include the weak interactions and the K sampling. At the $3 \times 3 \times 1/\Gamma$ and full $3 \times 3 \times 1$ levels, both PBE+D2 and OPTPBE functionals predict the same structure as the most stable one. The only exception is the acrylamide, although the stability difference is lower than the error of the method.

Our results also show that the adsorption energy is systematically overestimated by the PBE+D2 method with respect to the OPTPBE one in approximately 300 meV, regardless of the level. Since in Grimme’s D2 approach the dispersion is included through a semi-empirical way, whereas in OPTPBE it is included in the functional, OPTPBE results can be considered, in principle, more reliable. For the archetypal widely studied example of benzene on Cu(111), experimental values of adsorption energy are in the range 57 – 78 kJ/mol.^{70,106,107} PBE-D2 also overestimates the binding energy in this case 97 kJ/mol,¹⁰⁸ while vdW-DF slightly underestimates it (~ 53 kJ/mol).^{106,109}

The most stable structure in the three molecules (ACA-1, ACN-1 and ACO-3) shows a common characteristic: it always corresponds to a geometry with direct interaction between the C=C bond with a Cu atom on top position and also direct interaction between the N atom (ACN) or O atom (ACO and ACA) with a Cu atom on top position. This similarity confirms the nature of the interaction and can be considered as a general behavior.

The stability of the organic molecules on metal surfaces upon adsorption is crucial for

electronic nanodevices, since the coupling of the molecular states is effective only at short ranges, thus a strong anchoring (high E_{ads}) increases the efficiency of charge transfer through the linking sites.

Charge transfer

To go deep into the understanding of the metal-molecule interaction, we have also studied the charge transfer between molecule and surface upon adsorption (Δq). Several methods have been developed to evaluate atomic charges. Among them, the Mulliken population analysis (MPA),¹¹⁰ the Hirshfeld population analysis (HPA),¹¹¹ Quantum Theory of Atoms In Molecules (QTAIM),^{97,98} Natural Population Analysis (NPA),¹¹² and Voronoi Deformation Density method (VDD)¹¹³ are the most popular ones. They can yield drastically different absolute values¹¹⁴ and one has to be caution with the interpretation of the results. Our analysis have been carried out using the QTAIM method. The computed values of the transferred charge in the different adsorption geometries of each molecule are shown in Table 5.

Table 5: Transferred charge from the surface to the molecule (in atomic units) for the different molecules and adsorption geometries, computed at the level 2 (single point energy calculation with a 331 K-mesh over the geometry optimized with a Γ point).

| | PBE+D2 | OPTPBE |
|-------|--------|--------|
| ACA-1 | 0.264 | 0.188 |
| ACA-2 | 0.324 | 0.222 |
| ACN-1 | 0.369 | 0.286 |
| ACN-2 | 0.323 | 0.233 |
| ACO-1 | 0.573 | 0.496 |
| ACO-2 | 0.684 | 0.648 |
| ACO-3 | 0.478 | 0.416 |

We do not observe a clear relation between the charge transfer, Δq , and the adsorption energy. Acrolein is the molecule with the highest value of Δq , with a large difference with respect to the others, and its adsorption energy is located between that of acrylonitrile and acrylamide. There is no relation either between the different adsorption geometries of each molecule obtained with the two methods and Δq . Nevertheless, there is a clear trend in the

values: ACO has the greatest value in Δq , followed by ACN and being ACA the molecule that takes less charge transferred from the surface. This fact can be understood in terms of electronic structure; in particular analyzing the energies of the lowest unoccupied molecular orbital (LUMO) of each molecule in gas phase. The energy of this orbital with respect to the Fermi level is 1.47 eV in ACO; 1.69 eV in ACN and 2.14 eV in ACA. Thus a simple explanation arises: higher the electron affinity of the molecule larger the charge transferred from the surface.

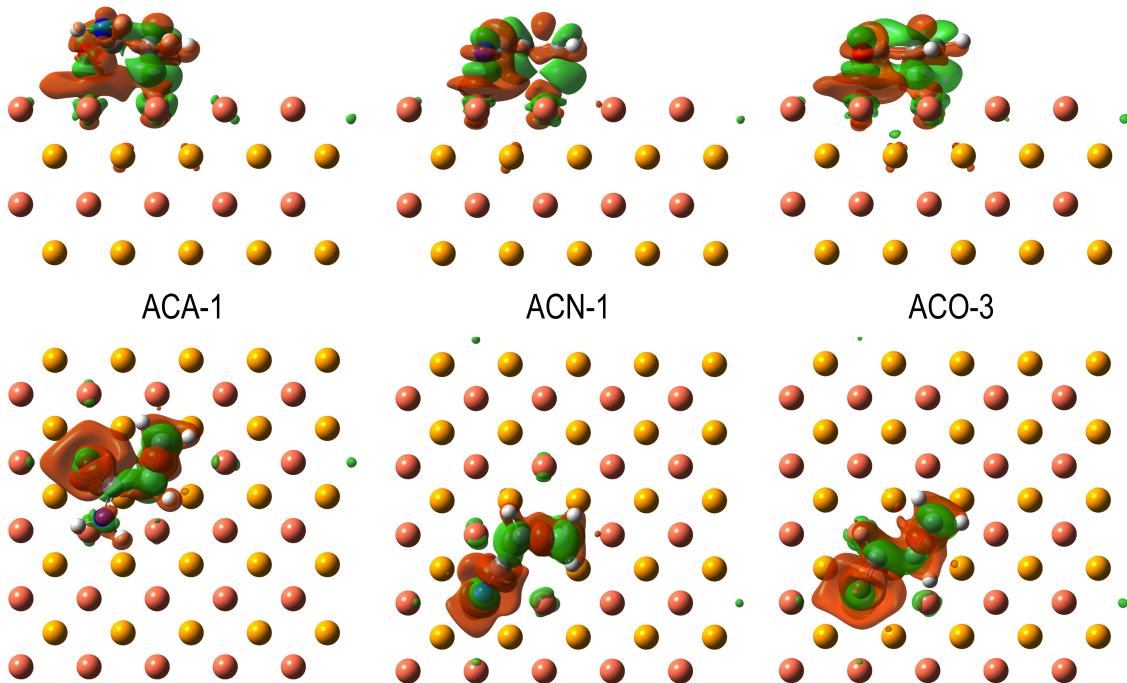


Figure 6: Change in the electronic density upon adsorption ($\Delta\rho$, isovalue=0.01) for the most stable adsorption structures of the three vinyl derivatives on Cu(100) surface. Green shows positive $\Delta\rho$ and Red negative $\Delta\rho$.

As in the analysis of the adsorption energies, the PBE+D2 functional gives higher values for Δq than the OPTPBE one. Since OPTPBE includes the weak interactions in the Hamiltonian (in the self-consistent optimization of the electronic density), charges given by this method should be more accurate. Consequently, the following analysis, related with the spatial redistribution of the electronic density, have been carried out using the OPTPBE

results. To this, we define the change in the electronic density upon adsorption as:

$$\Delta\rho = \rho_{molecule/surface} - (\rho_{molecule} + \rho_{surface}) \quad (2)$$

where $\rho_{molecule/surface}$ is the electronic density of the whole system, and $\rho_{molecule}$ and $\rho_{surface}$ are the densities of the molecule and surface computed keeping the adsorption geometry. The results (Fig. 6) reveal a high similarity between the regions where there is a gain of electronic density (in green) with the LUMO orbital of the corresponding molecule in the gas phase. It is reasonable to assume that, in the adsorption of these molecules on a Cu(100) surface the interaction leads to a charge transfer from the metal to the LUMO orbital of the molecule. The Δq regions also reflect the partial covalent character of the interactions, highlighting the linkage sites. The depletion of electron density in regions where there is no nodal plane in the π system, in addition to the mentioned gain in the LUMO, is explained in terms of a simple chemical picture: electron donation from the π orbital of the molecule to the surface and backdonation from the surface to the π^* orbital of the molecule (π -backbonding). We can also observe donation from lone pairs (LP) orbitals; typically from LP orbitals on the N atom in the cyano, and on the O atoms in the amide and carbonyl groups. Thus from the $\Delta\rho$ analysis we can infer $\pi \rightarrow \text{Cu}$ and $\text{LP} \rightarrow \text{Cu}$ donation and $\text{Cu} \rightarrow \pi^*$ backdonation. This phenomenon has been previously observed in a large variety of systems such as simple molecules,^{115–117} in organic molecules with aromatic rings and functional groups^{118,119} or in phthalocyanines¹²⁰ interacting with metal surfaces. The electronic structure analysis in the next section confirms this scenario.

The electronic properties of organic charge transfer (CT) compounds depend on the amount of charge transferred from the donor (D) to the acceptor (A) species. It has been shown that the CT process can be tuned by controlling the stoichiometry of the D and A quantities when they are forming self-assembled monolayers on metal surfaces¹²¹ and proceeds through the metal. Thus, the electron transport in hybrid organic-metal nanodevices

depends on the charge transfer efficiency.

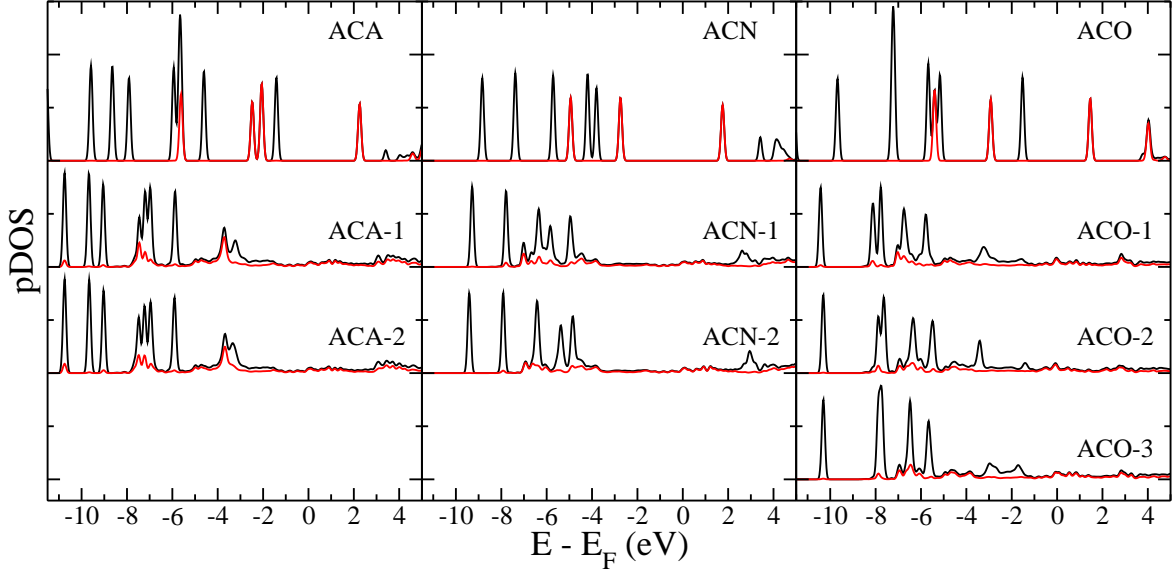


Figure 7: Density Of States projected on the atoms of the adsorbed molecules. Results of the molecule far from the slab, non interacting with the surface, is also shown for comparison - upper curves in each panel. In red, the pz-projection, which allows to identify the π contribution to the pDOS.

Electronic structure: energy levels alignment

Further information on the interaction nature is obtained by computing the projected Density Of States (pDOS). Decomposing the total Density Of States (DOS) in the contributions of the different angular momenta of each atom allows to analyze in detail the electronic structure and thus to determine the kind of interaction established between the molecule and the surface. For the different adsorption geometries of each molecule we present in Fig. 7 the DOS projected on all the atoms of the corresponding molecule. For comparison, the pDOS when the molecule is placed far enough from the surface to avoid interactions (typically $\sim 10\text{\AA}$), is presented as well in each case. The low energy region of the DOS is not shown because inner bands (which correspond to bonding σ molecular orbitals) barely change their position in energy after adsorption. They are just slightly shifted to lower energies due to

the transferred charge and are not relevant since they do not contribute to the linkage.

Comparing the pDOS of the molecules far from the slab with those interacting with the surface the main difference is found in the loss of resolution in the bands corresponding to the π and π^* orbitals in the isolated molecule and the lone pairs of the O and N: LP and π orbitals show the maximum hybridization with the metal states and are the responsible of the interaction. In general, broadening of the bands due to the interaction is observed also for other orbitals, although to a lesser extent. The observed change in the molecular states is a well known phenomenon¹²² and other theoretical works have previously pointed it out in the interaction of organic molecules with metal surfaces (see e.g.¹²³). Understanding this effect has consequences in the mechanisms that determine the optoelectronic properties of high-performance organic materials,¹²⁴ in particular in the rate of charge transfer between the active species (molecules) and the conductor (metal). As expected after the results obtained of the location of the transferred charge, the LUMO orbital of the three studied molecules is shifted below E_F becoming an occupied state with a bonding character and strongly contributes to the linkage of the molecule to the surface.¹⁶

A further analysis have been carried out by representing the change in the electronic density upon adsorption ($\Delta\rho$) in two-dimensional projections (see Figs. 8, 9 and 10). We obtain a complementary picture of the orbital hybridization due to the the charge transfer (mainly lone pair and π orbitals), i.e. the states involved in the donation/backdonation to/from the copper surface. Figure 8 shows 2D cuts of $\Delta\rho$ containing the π^* and the LP (O and N) orbitals of ACA. As previously mentioned, after the pDOS results, we observe an increase of the electronic density between C1 and C2 (backdonation from the surface to the π^*) and a depletion of the charge in the LP (dative interaction from the molecule to the surface). The charge transfer is higher in the oxygen than in the nitrogen atom, and can be simply explained in terms of distance, the NH_2 group is further away from the surface than the carbonyl (C=O) and therefore the interaction is less favored. As in the case of the ACA, the 2D cuts of ACO clearly show the dative interaction $\text{LP}_\text{O} \rightarrow \text{Cu}$ (depletion of the

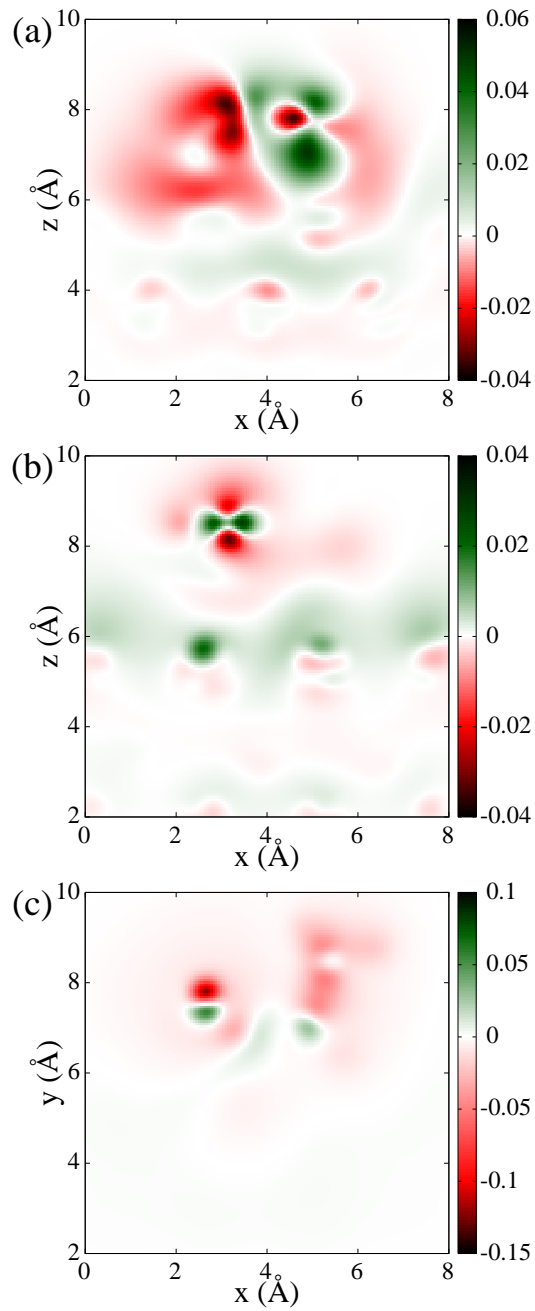


Figure 8: Two dimensional cuts of the change in the electronic density upon adsorption ($\Delta\rho$) in ACA-1: (a) xz plane located between C_1 and C_2 and shows the π^* density; (b)xz plane that contains the N atom and shows its lone pair orbital; (c) xy plane which contains the O atom and shows its lone pair orbital.

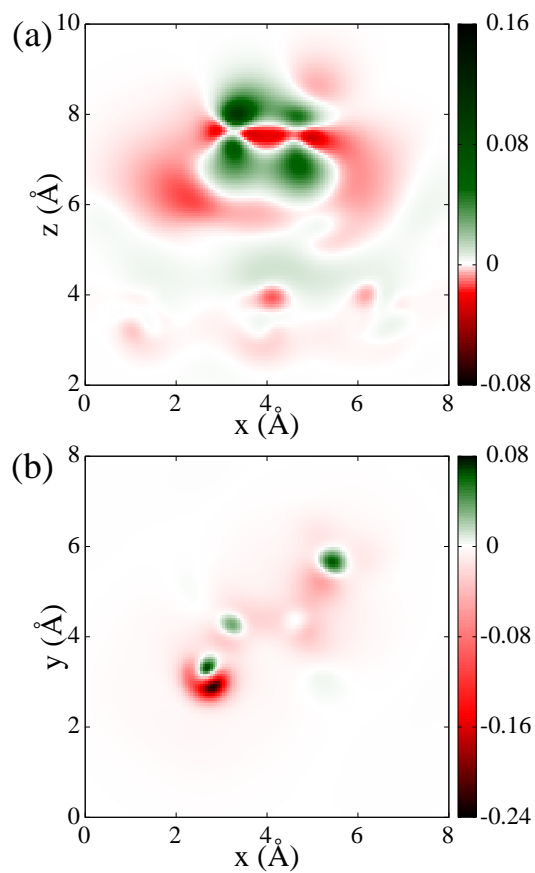


Figure 9: Two dimensional cuts of the change in the electronic density upon adsorption ($\Delta\rho$) in ACO-3: (a) xz plane located between C_1 and C_2 and shows the π^* orbital; (b) xy plane that contains the O atom and shows its lone pair orbital.

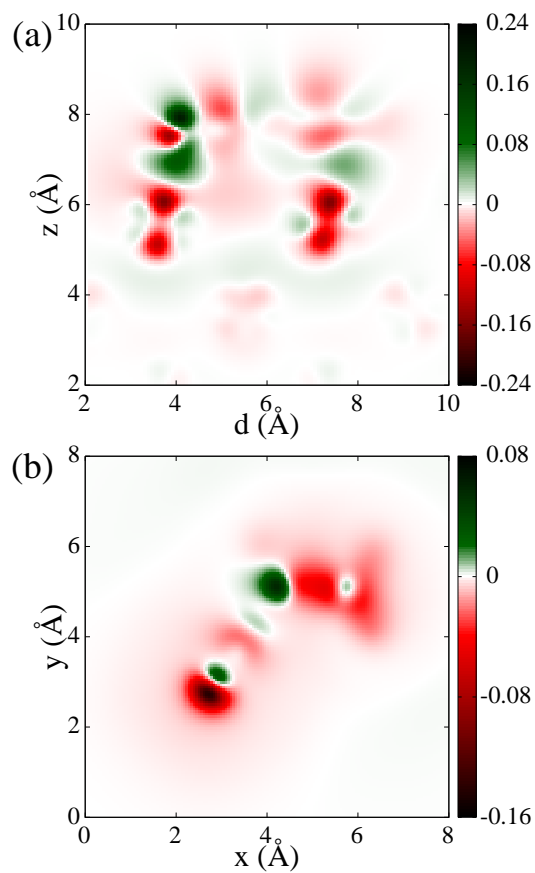


Figure 10: Two dimensional cuts of the change in the electronic density upon adsorption ($\Delta\rho$) in ACN-1: (a) xz plane located between C_1 and C_2 and shows the π^* orbital; (b) xy plane that contains the N atom and shows its lone pair orbital.

charge in the lone pair of the oxygen) and the backdonation from the Cu to the π^* (enhance of the electronic density in this orbital). Finally, ACN is very similar to ACA and ACO: the 2D cuts show that the electronic density in the region between C1 and C2 increases upon adsorption ($\text{Cu} \rightarrow \pi^*$), while the charge in the LP of the N atom decreases ($\text{LP}_\text{N} \rightarrow \text{Cu}$).

Conclusions

We have presented a detailed Density Functional Theory study of vinyl derivatives molecules (amide, aldehyde and cyano as substituents) adsorbed on a pristine Cu(100) surface. Our calculations also include periodic boundary conditions, in order to take into account a correct description of the metallic character of the surface. Weak interactions were included in the PBE functional through two different schemes: the Grimme’s D2 model and the OPT-DFT (OPTPBE). Differences in the results obtained with both methods mainly arise from the fact that D2 approach does not take into account the screening inside the metal and overestimates the interaction forces between the molecule and the metal surface. For the three organic molecules here studied, several stable structures were found, being these isomers almost degenerated in energy except in acrylonitrile, whose isomers have an energy difference of about 100 meV. In the three cases the most stable isomers have two common structural characteristics: the double C=C bond and an atom with a lone pair (oxygen in acrolein and acrylamide, and nitrogen in acrylonitrile) are placed on top position. This arrangement favors the interaction of the π orbital in the C=C bond of the molecule with the d orbital of the Cu atom, and the interaction of the lone-pair orbital in N and O with d orbitals of the Cu atom. The nature of the interaction between these molecules and the surface is verified with the analysis of the projected density of states and the charge transfer; both show a donation from the π_{CC} and from the lone pair orbitals to the surface and a backdonation to the π_{CC}^* orbital. This type of interaction and the relation between the energy of the LUMO orbital and the amount of transferred charge from the surface to the molecule seem to be a

common characteristic of the vinyl derivatives adsorbed on metal surfaces.

As a general conclusion, the interaction of organic molecules with π orbitals (typically in C=C double bonds) and lone pair orbitals (in Oxygen or Nitrogen atoms) are expected to interact with metal substrates with "d" orbitals in the manner we present in this work. The donation - backdonation is a synergic process that leads to the so called π -backbonding¹²⁵ and drives the adsorption of organic molecules in metal surfaces. The nature of the interactions described in this work might be also the responsible of the stabilization of small metal clusters surrounded by organic molecules^{126,127} and help in the synthesis of new metal-polymer nanocomposites.^{128,129}

Acknowledgement

We acknowledge the generous allocation of computer time at the Centro de Computación Científica at the Universidad Autónoma de Madrid (CCC-UAM) and the Red Española de Supercomputación (RES). This work was partially supported by the project CTQ2016-76061-P of the Spanish Ministerio de Economía y Competitividad (MINECO). F.A.G. acknowledges the FPI grant associated with the project CTQ2013-43698-P (MINECO). Financial support from the MINECO through the "María de Maeztu" Program for Units of Excellence in R&D (MDM-2014-0377) is also acknowledged.

References

- (1) Nørskov, J.; Bligaard, T.; Logadottir, A.; Bahn, S.; Hansen, L.; Bollinger, M.; Ben-gaard, H.; Hammer, B.; Sljivancanin, Z.; Mavrikakis, M.; Xu, Y.; Dahl, S.; Jacob-sen, C. Universality in Heterogeneous Catalysis. *J. Catal.* **2002**, *209*, 275 – 278.
- (2) Tauster, S. J.; Fung, S. C.; Baker, R. T. K.; Horsley, J. A. Strong Interactions in Supported-Metal Catalysts. *Science* **1981**, *211*, 1121–1125.

- (3) Muetterties, E. L. Metal Clusters in Catalysis III. - Clusters as Models for Chemisorption Processes and Heterogeneous Catalysis. *B. Soc. Chim. Belg.* **1975**, *84*, 959–986.
- (4) Bell, A. T. The Impact of Nanoscience on Heterogeneous Catalysis. *Science* **2003**, *299*, 1688–1691.
- (5) Moffat, J. *Theoretical Aspects of Heterogeneous Catalysis*; Van Nostrand Reinhold Electrical/Computer Science and Engineering Series; Springer Netherlands, 2013.
- (6) Joyner, R.; van Santen, R. *Elementary Reaction Steps in Heterogeneous Catalysis*; Nato Science Series C;; Springer Netherlands, 2012.
- (7) Salem, L. The mechanism of the chemical reaction, with recent developments pertaining to heterogeneous catalysis. *Int. J. Quantum Chem.* **1979**, *16*, 321–330.
- (8) Armbrust, N.; Schiller, F.; Gdde, J.; Hfer, U. Model potential for the description of metal/organic interface states. *Sci. Rep.-UK* **2017**, *7*, 46561.
- (9) Chen, S.; Zhao, Z.; Liu, H. Charge Transport at the Metal-Organic Interface. *Ann. Rev. Phys. Chem.* **2013**, *64*, 221–245.
- (10) Scott, J. C. Metal-Organic interface and charge injection in organic electronic devices. *J. Vac. Sci. Technol. A* **2003**, *21*, 521–531.
- (11) Hwang, J.; Wan, A.; Kahn, A. Energetics of metal-organic interfaces: New experiments and assessment of the field. *Mat. Sci. Eng. R* **2009**, *64*, 1 – 31.
- (12) Zaworotko, M. J. A reversible step forward. *Nat. Chem.* **2009**, *1*, 267.
- (13) Furukawa, H.; Cordova, K. E.; O’Keeffe, M.; Yaghi, O. M. The Chemistry and Applications of Metal-Organic Frameworks. *Science* **2013**, *341*.
- (14) Zhou, H.-C.; Long, J. R.; Yaghi, O. M. Introduction to Metal-Organic Frameworks. *Chem. Rev.* **2012**, *112*, 673–674.

- (15) Sánchez, C.; Julian, B.; Belleville, P.; Popall, M. Applications of hybrid organic-inorganic nanocomposites. *J. Mater. Chem.* **2005**, *15*, 3559–3592.
- (16) Ishii, H.; Sugiyama, K.; Ito, E.; Seki, K. Energy Level Alignment and Interfacial Electronic Structures at Organic/Metal and Organic/Organic Interfaces. *Adv. Mater.* **1999**, *11*, 605–625.
- (17) Ferey, G. Hybrid porous solids: past, present, future. *Chem. Soc. Rev.* **2008**, *37*, 191–214.
- (18) Yu, G.; Gao, J.; Hummelen, J. C.; Wudl, F.; Heeger, A. J. Polymer Photovoltaic Cells: Enhanced Efficiencies via a Network of Internal Donor-Acceptor Heterojunctions. *Science* **1995**, *270*, 1789–1791.
- (19) Günes, S.; Neugebauer, H.; Sariciftci, N. S. Conjugated Polymer-Based Organic Solar Cells. *Chem. Rev.* **2007**, *107*, 1324–1338.
- (20) Tang, C. W. Two-layer organic photovoltaic cell. *Appl. Phys. Lett.* **1986**, *48*, 183–185.
- (21) Grätzel, M. Dye-sensitized solar cells. *J. Photoch. PhotoBio. C* **2003**, *4*, 145 – 153.
- (22) Saragi, T. P. I.; Spehr, T.; Siebert, A.; Fuhrmann-Lieker, T.; Salbeck, J. Spiro Compounds for Organic Optoelectronics. *Chem. Rev.* **2007**, *107*, 1011–1065.
- (23) Shekhah, O.; Liu, J.; Fischer, R. A.; Woll, C. MOF thin films: existing and future applications. *Chem. Soc. Rev.* **2011**, *40*, 1081–1106.
- (24) Choy, K. Chemical vapour deposition of coatings. *Prog. Mat. Sci.* **2003**, *48*, 57 – 170.
- (25) Sirringhaus, H.; Tessler, N.; Friend, R. H. Integrated Optoelectronic Devices Based on Conjugated Polymers. *Science* **1998**, *280*, 1741–1744.
- (26) Rogers, J. A.; Someya, T.; Huang, Y. Materials and Mechanics for Stretchable Electronics. *Science* **2010**, *327*, 1603–1607.

- (27) Law, M.; Greene, L. E.; Johnson, J. C.; Saykally, R.; Yang, P. Nanowire dye-sensitized solar cells. *Nat. Mater.* **2005**, *4*, 455.
- (28) Hagfeldt, A.; Boschloo, G.; Sun, L.; Kloo, L.; Pettersson, H. Dye-Sensitized Solar Cells. *Chem. Rev.* **2010**, *110*, 6595–6663.
- (29) Bogani, L.; Wernsdorfer, W. Molecular spintronics using single-molecule magnets. *Nat. Mater.* **2008**, *7*, 179.
- (30) Rocha, A. R.; Garcia-Suarez, V. M.; Bailey, S. W.; Lambert, C. J.; Ferrer, J.; Sanvito, S. Towards molecular spintronics. *Nat. Mater.* **2005**, *4*, 335.
- (31) Sanvito, S. Molecular spintronics. *Chem. Soc. Rev.* **2011**, *40*, 3336–3355.
- (32) Mannini, M.; Pineider, F.; Sainctavit, P.; Danieli, C.; Otero, E.; Sciancalepore, C.; Talarico, A. M.; Arrio, M.-A.; Cornia, A.; Gatteschi, D.; Sessoli, R. Magnetic memory of a single-molecule quantum magnet wired to a gold surface. *Nat. Mater.* **2009**, *8*, 194.
- (33) Gray, J.; Luan, B. Protective coatings on magnesium and its alloys - a critical review. *J. Alloy. Compd.* **2002**, *336*, 88 – 113.
- (34) Huber, D. L. Synthesis, Properties, and Applications of Iron Nanoparticles. *Small* **2005**, *1*, 482–501.
- (35) Chung, I.; Lee, B.; He, J.; Chang, R. P. H.; Kanatzidis, M. G. All-solid-state dye-sensitized solar cells with high efficiency. *Nature* **2012**, *485*, 486.
- (36) Hakkinen, H. The gold-sulfur interface at the nanoscale. *Nat. Chem.* **2012**, *4*, 443.
- (37) Tautz, F. Structure and bonding of large aromatic molecules on noble metal surfaces: The example of PTCDA. *Prog. Surf. Sci.* **2007**, *82*, 479 – 520.

- (38) Temprano, I.; Thomas, G.; Haq, S.; Dyer, M. S.; Latter, E. G.; Darling, G. R.; Uvdal, P.; Raval, R. 1D self-assembly of chemisorbed thymine on Cu(110) driven by dispersion forces. *J. Chem. Phys.* **2015**, *142*, 101916.
- (39) Schreiber, F. Structure and growth of self-assembling monolayers. *Prog. Surf. Sci.* **2000**, *65*, 151 – 257.
- (40) Templeton, A. C.; Wuelfing, W. P.; Murray, R. W. Monolayer-Protected Cluster Molecules. *Accounts Chem. Res.* **2000**, *33*, 27–36.
- (41) Love, J. C.; Estroff, L. A.; Kriebel, J. K.; Nuzzo, R. G.; Whitesides, G. M. Self-Assembled Monolayers of Thiolates on Metals as a Form of Nanotechnology. *Chem. Rev.* **2005**, *105*, 1103–1170.
- (42) Ulman, A. Formation and Structure of Self-Assembled Monolayers. *Chem. Rev.* **1996**, *96*, 1533–1554.
- (43) Dubois, L. H.; Nuzzo, R. G. Synthesis, Structure, and Properties of Model Organic Surfaces. *Annu. Rev. Phys. Chem.* **1992**, *43*, 437–463.
- (44) Bin, H.; Yang, Y.; Zhang, Z.-G.; Ye, L.; Ghasemi, M.; Chen, S.; Zhang, Y.; Zhang, C.; Sun, C.; Xue, L.; Yang, C.; Ade, H.; Li, Y. 9.73% Efficiency Nonfullerene All Organic Small Molecule Solar Cells with Absorption-Complementary Donor and Acceptor. *J. Am. Chem. Soc.* **2017**, *139*, 5085–5094.
- (45) Díaz-Tendero, S.; Alcamí, M.; Martín, F. Density functional theory study of the structure and vibrational modes of acrylonitrile adsorbed on Cu(100). *Phys. Chem. Chem. Phys.* **2013**, *15*, 1288–1295.
- (46) Meyer, R.; Lemire, C.; Shaikhutdinov, S. K.; Freund, H. J. Surface chemistry of catalysis by gold. *Gold Bull.* **2004**, *37*, 72–124.

- (47) Yang, M. X.; Eng, J.; Kash, P. W.; Flynn, G. W.; Bent, B. E.; Holbrook, M. T.; Bare, S. R.; Gland, J. L.; Fischer, D. A. Generation and Reaction of Vinyl Groups on a Cu(100) Surface. *J. Phys. Chem.* **1996**, *100*, 12431–12439.
- (48) Gurevich, A. B.; Teplyakov, A. V.; Yang, M. X.; Bent, B. E.; Holbrook, M. T.; Bare, S. R. Synthesis, Bonding, and Reactions of pi-Bonded Allyl Groups on Cu(100): Allyl Radical Ejection. *Langmuir* **1998**, *14*, 1419–1427.
- (49) Lin, J.-L.; Lin, H.-P.; Yang, C.-M.; Chen, T.-Y.; Lee, S.-H.; Chiang, C.-M. Reactions of CH₂=CHBr and CH₃CHBr₂ on Cu(100) and O/Cu(100). *J. Phys. Chem. C* **2017**, *121*, 17990–17998.
- (50) Voigtländer, B. *Scanning Probe Microscopy: Atomic Force Microscopy and Scanning Tunneling Microscopy*; NanoScience and Technology; Springer Berlin Heidelberg, 2015.
- (51) Butt, H.-J.; Cappella, B.; Kappl, M. Force measurements with the atomic force microscope: Technique, interpretation and applications. *Surf. Sci. Rep.* **2005**, *59*, 1 – 152.
- (52) Binnig, G.; Rohrer, H.; Gerber, C.; Weibel, E. Surface Studies by Scanning Tunneling Microscopy. *Phys. Rev. Lett.* **1982**, *49*, 57–61.
- (53) Stroscio, J. A., Kaiser, W. J., Eds. *Scanning Tunneling Microscopy*; Academic Press: San Diego, 1993; p ii.
- (54) Meyer, E.; Hug, H. J.; Bennewitz, R. *Scanning Probe Microscopy: The Lab on a Tip*; Springer Berlin Heidelberg: Berlin, Heidelberg, 2004; pp 15–44.
- (55) Zegenhagen, J.; Kazimirov, A. *The X-Ray Standing Wave Technique*; WORLD SCIENTIFIC, 2013.

- (56) Woodruff, D. Surface structural information from photoelectron diffraction. *J. Electron. Spectros. Relat. Phenom.* **2010**, 178-179, 186 – 194, Trends in X-ray Photoelectron Spectroscopy of solids (theory, techniques and applications).
- (57) Hüfner, S. *Photoelectron Spectroscopy: Principles and Applications*; Springer Berlin Heidelberg: Berlin, Heidelberg, 2003; pp 597–634.
- (58) Rakić, V.; Damjanović, L. In *Calorimetry and Thermal Methods in Catalysis*; Auroux, A., Ed.; Springer Berlin Heidelberg: Berlin, Heidelberg, 2013; pp 131–174.
- (59) Falconer, J. L.; Schwarz, J. A. Temperature-Programmed Desorption and Reaction: Applications to Supported Catalysts. *Cataly. Rev.* **1983**, 25, 141–227.
- (60) Nefedov, V.; Shartse, N. *X-Ray Photoelectron Spectroscopy of Solid Surfaces*; Taylor & Francis, 1988.
- (61) Briggs, D.; Seah, M. *Practical Surface Analysis, Auger and X-ray Photoelectron Spectroscopy*; Practical Surface Analysis; Wiley, 1996.
- (62) Liu, W.; Tkatchenko, A.; Scheffler, M. Modeling Adsorption and Reactions of Organic Molecules at Metal Surfaces. *Accounts Chem. Res.* **2014**, 47, 3369–3377.
- (63) Chulkov, E. V.; Borisov, A. G.; Gauyacq, J. P.; Sánchez-Portal, D.; Silkin, V. M.; Zhukov, V. P.; Echenique, P. M. Electronic Excitations in Metals and at Metal Surfaces. *Chem. Rev.* **2006**, 106, 4160–4206.
- (64) Nilsson, A.; Pettersson, L. G.; Nørskov, J. K. In *Chemical Bonding at Surfaces and Interfaces*; Nilsson, A., Pettersson, L. G., Nørskov, J. K., Eds.; Elsevier: Amsterdam, 2008; pp xi – xii.
- (65) Díaz-Tendero, S.; Borisov, A. G.; Gauyacq, J.-P. Theoretical study of the electronic excited states in ultrathin ionic layers supported on metal surfaces: NaCl/Cu(111). *Phys. Rev. B* **2011**, 83, 115453.

- (66) Díaz-Tendero, S.; Foelsch, F. E.; Stefan aoe Olsson; Borisov, A. G.; Gauyacq, J.-P. Electron Propagation along Cu Nanowires Supported on a Cu(111) Surface. *Nano Lett.* **2008**, *8*, 2712–2717.
- (67) Díaz-Tendero, S.; Borisov, A. G.; Gauyacq, J.-P. Extraordinary Electron Propagation Length in a Metallic Double Chain Supported on a Metal Surface. *Phys. Rev. Lett.* **2009**, *102*, 166807.
- (68) Chiter, F.; Nguyen, V. B.; Tarrat, N.; Benoit, M.; Tang, H.; Lacaze-Dufaure, C. Effect of van der Waals corrections on DFT-computed metallic surface properties. *Mater. Res. Express* **2016**, *3*, 046501.
- (69) Andersson, Y.; Hult, E.; Rydberg, H.; Apell, P.; Lundqvist, B. I.; Langreth, D. C. In *Electronic Density Functional Theory: Recent Progress and New Directions*; Dobson, J. F., Vignale, G., Das, M. P., Eds.; Springer US: Boston, MA, 1998; pp 243–260.
- (70) Ruiz, V. G.; Liu, W.; Zojer, E.; Scheffler, M.; Tkatchenko, A. Density-Functional Theory with Screened van der Waals Interactions for the Modeling of Hybrid Inorganic-Organic Systems. *Phys. Rev. Lett.* **2012**, *108*, 146103.
- (71) Ruiz, V. G.; Liu, W.; Tkatchenko, A. Density-functional theory with screened van der Waals interactions applied to atomic and molecular adsorbates on close-packed and non-close-packed surfaces. *Phys. Rev. B* **2016**, *93*, 035118.
- (72) Berland, K.; Cooper, V. R.; Lee, K.; Schröder, E.; Thonhauser, T.; Hyldgaard, P.; Lundqvist, B. I. van der Waals forces in density functional theory: a review of the vdW-DF method. *Rep. Prog. Phys.* **2015**, *78*, 066501.
- (73) Robledo, M.; Díaz-Tendero, S. Exploring the Adsorption and the Potential Energy Surface of Acrylonitrile on Cu(100) and Cu(100) Coated with NaCl Layers. *J. Phys. Chem. C* **2015**, *119*, 15125–15136.

- (74) Robledo, M.; Pacchioni, G.; Martín, F.; Alcamí, M.; Díaz-Tendero, S. Adsorption of Benzene on Cu(100) and on Cu(100) Covered with an Ultrathin NaCl Film: Molecule-Substrate Interaction and Decoupling. *J. Phys. Chem. C* **2015**, *119*, 4062–4071.
- (75) Grimme, S. Accurate description of van der Waals complexes by density functional theory including empirical corrections. *J. Comp. Chem.* **2004**, *25*, 1463–1473.
- (76) Grimme, S. Semiempirical GGA-type density functional constructed with a long-range dispersion correction. *J. Comp. Chem.* **2006**, *27*, 1787–1799.
- (77) Grimme, S.; Antony, J.; Ehrlich, S.; Krieg, H. A consistent and accurate ab initio parametrization of density functional dispersion correction (DFT-D) for the 94 elements H-Pu. *J. Chem. Phys.* **2010**, *132*, 154104.
- (78) Dion, M.; Rydberg, H.; Schröder, E.; Langreth, D. C.; Lundqvist, B. I. Van der Waals Density Functional for General Geometries. *Phys. Rev. Lett.* **2004**, *92*, 246401.
- (79) Klimeš, J. c. v.; Bowler, D. R.; Michaelides, A. Van der Waals density functionals applied to solids. *Phys. Rev. B* **2011**, *83*, 195131.
- (80) Román-Pérez, G.; Soler, J. M. Efficient Implementation of a van der Waals Density Functional: Application to Double-Wall Carbon Nanotubes. *Phys. Rev. Lett.* **2009**, *103*, 096102.
- (81) Berland, K.; Hyldgaard, P. Exchange functional that tests the robustness of the plasmon description of the van der Waals density functional. *Phys. Rev. B* **2014**, *89*, 035412.
- (82) Berland, K.; Arter, C. A.; Cooper, V. R.; Lee, K.; Lundqvist, B. I.; Schroder, E.; Thonhauser, T.; Hyldgaard, P. van der Waals density functionals built upon the electron-gas tradition: Facing the challenge of competing interactions. *J. Chem. Phys.* **2014**, *140*, 18A539.

- (83) Becke, A. D.; Johnson, E. R. Exchange-hole dipole moment and the dispersion interaction. *J. Chem. Phys.* **2005**, *122*, 154104.
- (84) Kannemann, F. O.; Becke, A. D. van der Waals Interactions in Density-Functional Theory: Intermolecular Complexes. *J. Chem. Theory Comput.* **2010**, *6*, 1081–1088.
- (85) Steinmann, S. N.; Corminboeuf, C. Comprehensive Benchmarking of a Density-Dependent Dispersion Correction. *J. Chem. Theory Comput.* **2011**, *7*, 3567–3577.
- (86) Tkatchenko, A.; Scheffler, M. Accurate Molecular Van Der Waals Interactions from Ground-State Electron Density and Free-Atom Reference Data. *Phys. Rev. Lett.* **2009**, *102*, 073005.
- (87) Maurer, R. J.; Ruiz, V. G.; Camarillo-Cisneros, J.; Liu, W.; Ferri, N.; Reuter, K.; Tkatchenko, A. Adsorption structures and energetics of molecules on metal surfaces: Bridging experiment and theory. *Progress in Surface Science* **2016**, *91*, 72 – 100.
- (88) Mercurio, G.; McNellis, E. R.; Martin, I.; Hagen, S.; Leyssner, F.; Soubatch, S.; Meyer, J.; Wolf, M.; Tegeder, P.; Tautz, F. S.; Reuter, K. Structure and Energetics of Azobenzene on Ag(111): Benchmarking Semiempirical Dispersion Correction Approaches. *Phys. Rev. Lett.* **2010**, *104*, 036102.
- (89) Sony, P.; Puschnig, P.; Nabok, D.; Ambrosch-Draxl, C. Importance of Van Der Waals Interaction for Organic Molecule-Metal Junctions: Adsorption of Thiophene on Cu(110) as a Prototype. *Phys. Rev. Lett.* **2007**, *99*, 176401.
- (90) Mura, M.; Gulans, A.; Thonhauser, T.; Kantorovich, L. Role of van der Waals interaction in forming molecule-metal junctions: flat organic molecules on the Au(111) surface. *Phys. Chem. Chem. Phys.* **2010**, *12*, 4759–4767.
- (91) Li, G.; Tamblyn, I.; Cooper, V. R.; Gao, H.-J.; Neaton, J. B. Molecular adsorption

- on metal surfaces with van der Waals density functionals. *Phys. Rev. B* **2012**, *85*, 121409.
- (92) Bilic, A.; Reimers, J. R.; Hush, N. S. Adsorption of Pyridine on the Gold(111) Surface: Implications for Alligator Clips for Molecular Wires. *J. Phys. Chem. B* **2002**, *106*, 6740–6747.
- (93) Kresse, G.; Furthmüller, J. Efficiency of ab-initio total energy calculations for metals and semiconductors using a plane-wave basis set. *Comput. Mat. Sci.* **1996**, *6*, 15–50.
- (94) Kresse, G.; Furthmüller, J. Efficient iterative schemes for ab initio total-energy calculations using a plane-wave basis set. *Phys. Rev. B* **1996**, *54*, 11169.
- (95) Perdew, J. P.; Burke, K.; Ernzerhof, M. Generalized Gradient Approximation Made Simple. *Phys. Rev. Lett.* **1996**, *77*, 3865–3868.
- (96) Klimeš, J. c. v.; Bowler, D. R.; Michaelides, A. Chemical accuracy for the van der Waals density functional. *J. Phys.-Condens. Mat.* **2010**, *22*, 022201.
- (97) Bader, R. F. W. A quantum theory of molecular structure and its applications. *Chem. Rev.* **1991**, *91*, 893–928.
- (98) Bader, R. F. W. *Atoms in Molecules: A Quantum Theory*; Oxford University Press, USA, 1994.
- (99) Tang, W.; Sanville, E.; Henkelman, G. A grid-based Bader analysis algorithm without lattice bias. *J. Phys. Condens. Mat.* **2009**, *21*, 084204.
- (100) Sanville, E.; Kenny, S. D.; Smith, R.; Henkelman, G. Improved grid-based algorithm for Bader charge allocation. *J. Comput. Chem.* **2007**, *28*, 899–908.
- (101) Henkelman, G.; Arnaldsson, A.; Jonsson, H. A fast and robust algorithm for Bader decomposition of charge density. *Comp. Mat. Sci.* **2006**, *36*, 354 – 360.

- (102) Geskin, V. M.; Lazzaroni, R.; Mertens, M.; Jérôme, R.; Brédas, J. L. Acrylonitrile on Cu(100): A density functional theoretical study of adsorption and electrochemical grafting. *J. Chem. Phys.* **1996**, *105*, 3278–3289.
- (103) Crispin, X.; Bureau, C.; Geskin, V. M.; Lazzaroni, R.; Salaneck, W. R.; Brédas, J. L. Chemisorption of acrylonitrile on the Cu(100) surface: A local density functional study. *J. Chem. Phys.* **1999**, *111*, 3237–3251.
- (104) Crispin, X.; Geskin, V.; Crispin, A.; Cornil, J.; Lazzaroni, R.; Salaneck, W. R.; Brédas, J.-L. Characterization of the Interface Dipole at Organic/ Metal Interfaces. *J. Am. Chem. Soc.* **2002**, *124*, 8131–8141.
- (105) Carrasco, J.; Liu, W.; Michaelides, A.; Tkatchenko, A. Insight into the description of van der Waals forces for benzene adsorption on transition metal (111) surfaces. *J. Chem. Phys.* **2014**, *140*, 084704.
- (106) Lukas, S.; Vollmer, S.; Witte, G.; Woll, C. Adsorption of acenes on flat and vicinal Cu(111) surfaces: Step induced formation of lateral order. *J. Chem. Phys.* **2001**, *114*, 10123–10130.
- (107) Klimeš, J. c. v.; Michaelides, A. Perspective: Advances and challenges in treating van der Waals dispersion forces in density functional theory. *J. Chem. Phys.* **2012**, *137*, 120901.
- (108) McNellis, E. R.; Meyer, J.; Reuter, K. Azobenzene at coinage metal surfaces: Role of dispersive van der Waals interactions. *Phys. Rev. B* **2009**, *80*, 205414.
- (109) Berland, K.; Einstein, T. L.; Hyldgaard, P. Rings sliding on a honeycomb network: Adsorption contours, interactions, and assembly of benzene on Cu(111). *Phys. Rev. B* **2009**, *80*, 155431.

- (110) Mulliken, R. S. Electronic Population Analysis on LCAO-MO Molecular Wave Functions. I. *J. Chem. Phys.* **1955**, *23*, 1833–1840.
- (111) Hirshfeld, F. L. Bonded-atom fragments for describing molecular charge densities. *Theor. Chim. Acta* **1977**, *44*, 129–138.
- (112) Reed, A. E.; Weinstock, R. B.; Weinhold, F. Natural population analysis. *J. Chem. Phys.* **1985**, *83*, 735–746.
- (113) Fonseca Guerra, C.; Handgraaf, J.-W.; Baerends, E. J.; Bickelhaupt, F. M. Voronoi deformation density (VDD) charges: Assessment of the Mulliken, Bader, Hirshfeld, Weinhold, and VDD methods for charge analysis. *J. Comput. Chem.* **2004**, *25*, 189–210.
- (114) Wiberg, K. B.; Rablen, P. R. Comparison of atomic charges derived via different procedures. *J. Comput. Chem.* **1993**, *14*, 1504–1518.
- (115) Reguera, E. Materials for Hydrogen Storage in Nanocavities: Design criteria. *Int. J. Hydrogen Energ.* **2009**, *34*, 9163 – 9167.
- (116) Gladh, J.; Öberg, H.; Li, J.; Ljungberg, M. P.; Matsuda, A.; Ogasawara, H.; Nilsson, A.; Pettersson, L. G. M.; Öström, H. X-ray emission spectroscopy and density functional study of CO/Fe(100). *J. Chem. Phys.* **2012**, *136*, 034702.
- (117) Dell’Angela, M. et al. Real-Time Observation of Surface Bond Breaking with an X-ray Laser. *Science* **2013**, *339*, 1302–1305.
- (118) Verma, C. B.; Quraishi, M.; Singh, A. 2-Aminobenzene-1,3-dicarbonitriles as green corrosion inhibitor for mild steel in 1 M HCl: Electrochemical, thermodynamic, surface and quantum chemical investigation. *J. Taiwan Inst. Chem. E.* **2015**, *49*, 229 – 239.
- (119) Simpson, S.; Hooper, J.; Miller, D. P.; Kunkel, D. A.; Enders, A.; Zurek, E. Modulating Bond Lengths via Backdonation: A First-Principles Investigation of a Quinonoid

- Zwitterion Adsorbed to Coinage Metal Surfaces. *J. Phys. Chem. C* **2016**, *120*, 6633–6641.
- (120) Toader, M.; Shukryna, P.; Knupfer, M.; Zahn, D. R. T.; Hietschold, M. Site-Dependent Donation/Backdonation Charge Transfer at the CoPc/Ag(111) Interface. *Langmuir* **2012**, *28*, 13325–13330.
- (121) Rodriguez-Fernandez, J. et al. Tuning Intermolecular Charge Transfer in Donor-Acceptor Two-Dimensional Crystals on Metal Surfaces. *J. Phys. Chem. C* **2017**, *121*, 23505–23510.
- (122) Zangwill, A. *Physics at Surfaces*; Cambridge University Press, 1988.
- (123) Vazquez, H.; Flores, F.; Oszwaldowski, R.; Ortega, J.; Perez, R.; Kahn, A. Barrier formation at metal-organic interfaces: dipole formation and the charge neutrality level. *Appl. Surf. Sci.* **2004**, *234*, 107 – 112.
- (124) Ostroverkhova, O. Organic Optoelectronic Materials: Mechanisms and Applications. *Chem. Rev.* **2016**, *116*, 13279–13412.
- (125) Cotton, F. *Advanced Inorganic Chemistry*; A Wiley-Interscience Publication; Wiley, 1999.
- (126) Lewis, L. N. Chemical catalysis by colloids and clusters. *Chem. Rev.* **1993**, *93*, 2693–2730.
- (127) Schmid, G.; Maihack, V.; Lantermann, F.; Peschel, S. Ligand-stabilized metal clusters and colloids: properties and applications. *J. Chem. Soc., Dalton Trans.* **1996**, 589–595.
- (128) Raveendran, P.; Fu, J.; Wallen, S. L. Completely Green Synthesis and Stabilization of Metal Nanoparticles. *J. Am. Chem. Soc.* **2003**, *125*, 13940–13941.
- (129) Nicolais, L.; Carotenuto, G. *Metal-Polymer Nanocomposites*; Wiley, 2004.

Graphical TOC Entry

